High speed, high power one-dimensional beam steering from a 6-element optical phased array

W. Ronny Huang,* Juan Montoya, Jan E. Kansky, Shawn M. Redmond, George W. Turner, and Antonio Sanchez-Rubio

Lincoln Laboratory, Massachusetts Institute of Technology, Lexington, Massachusetts 02420, USA

*we21748@mit.edu

Abstract: Beam steering at high speed and high power is demonstrated from a 6-element optical phased array using coherent beam combining (CBC) techniques. The steering speed, defined as the inverse of the time to required to sweep the beam across the steering range, is 40 MHz and the total power is 396 mW. The measured central lobe FWHM width is 565 μrad. High on-axis intensity is maintained periodically by phase-locking the array via a stochastic-parallel-gradient-descent (SPGD) algorithm. A master-oscillator-power-amplifier (MOPA) configuration is used where the amplifier array elements are semiconductor slab-coupled-optical-waveguide-amplifiers (SCOWAs). The beam steering is achieved by $LiNbO_3$ phase modulators; the phase-locking occurs by current adjustment of the SCOWAs. The system can be readily scaled to GHz steering speed and multiwatt-class output.

OCIS codes: (140.2010) Diode laser arrays; (140.3298) Laser beam combining.

References and links

1. P. F. McManamon, P. J. Bos, M. J. Escuti, J. Heikenfeld, S. Serati, H. Xie, and E. A. Watson, "A review of phased array steering for narrow-band electrooptical systems," Proc. IEEE **97**, 1078–1096 (2009).
2. D. Kwong, A. Hosseini, Y. Zhang, and R. T. Chen, "Unequally spaced waveguide array for actively tuned optical phased array on a silicon nanomembrane," Appl. Phys. Lett. **99**, 051104 (2011).
3. K. Van Acoleyen, H. Rogier, and R. Baets, "Two-dimensional optical phased array antenna on silicon-on-insulator," Opt. Express **18**, 13655–13660 (2010).
4. K. Van Acoleyen, W. Bogaerts, and R. Baets, "Two-dimensional dispersive on-chip beam scanner fabricated on silicon-on-insulator," IEEE Photon. Technol. Lett. **23**, 1270–1272 (2011).
5. J. K. Doylend, M. J. R. Heck, J. T. Bovington, J. D. Peters, L. A. Coldren, and J. E. Bowers, "Two-dimensional free-space beam steering with an optical phased array on silicon-on-insulator," Opt. Express **19**, 21595–21604 (2011).
6. Y. Vilenchik, B. I. Erkmen, N. Satyan, A. Yariv, W. H. Farr, and J. M. Choi, "Optical phase lock loop based phased array transmitter for optical communications," The Interplanetary Network Progress Report **42-184**, C (2011).
7. M. Jarrahi, R. Fabian, W. Pease, D. A. B. Miller, and T. H. Lee, "High-speed optical beam-steering based on phase-arrayed waveguides," Am. Vac. Soc. **26**, 2124–2126 (2008).
8. J. P. Donnelly, R. K. Huang, J. N. Walpole, L. J. Missaggia, C. T. Harris, J. J. Plant, R. J. Bailey, D. E. Mull, W. D. Goodhue, and G. W. Turner, "AlGaAs-InGaAs slab-coupled optical waveguide lasers," IEEE J. Quantum Electron. **39**, 289–298 (2003).
9. M. A. Vorontsov and V. P. Sivokon, "Stochastic parallel-gradient-descent technique for high-resolution wavefront phase-distortion correction," J. Opt. Soc. Am. A **15**, 2745–2758 (1998).

#167785 - $15.00 USD Received 1 May 2012; revised 8 Jun 2012; accepted 12 Jun 2012; published 16 Jul 2012

10. J. E. Kansky, C. X. Yu, D. V. Murphy, S. E. J. Shaw, R. C. Lawrence, and C. Higgs, "Uncooperative target-in-the-loop performance with backscattered speckle-field effects," Proc. SPIE **6306**, 63060G (2007).
11. T. Y. Fan, "The effect of amplitude (power) variations on beam combining efficiency for phased arrays," IEEE J. Sel. Top. Quantum Electron. **15**, 291–293 (2009).

1. Introduction

Rapid and precise beam steering is a crucial element in free-space optical applications which require random-access pointing and agile stabilization. Traditional mechanical steering approaches, such as the dual-axis gimbaled mirror, suffer from high power consumption and slow speed. These limitations have fueled the development of optical phased array (OPA) technology for beam steering without moving parts. The classic OPA approach of transmitting a beam through an array of liquid crystal (LC) phase shifters [1] is proven and mature, but LC cells have slow response times ($\sim$kHz) and limited steering angles. More recently, fully-integrated one-dimensional OPAs with unequal spacing utilizing phase tuning [2] and two-dimensional OPAs utilizing wavelength [3, 4] and both wavelength and phase [5] tuning have demonstrated large-angle steering but are still limited in steering speed ($\sim$100 kHz) and output power ($\sim$mW). High speed beam steering systems have been developed using optical phase lock loops [6] and phased waveguides [7], but these experiments have yet to be scaled beyond 2 elements and to watt-class power, respectively.

In this report, we present high power output from a 6-element OPA, with fast steering speed (defined as the inverse of the time to required to sweep the beam across the steering range). This scheme uses a narrow-linewidth source to seed an array of slab-coupled-waveguide semiconductor amplifiers (SCOWAs) [8]. Each SCOWA is capable of producing a diffraction-limited beam with power of up to 1 W. Dephasing occurring from non-common optical path drift between array elements is mitigated by periodically toggling between a phase-lock cycle and a beam steering cycle. During the phase-lock cycle, the phases are synchronized via a stochastic-parallel-gradient-descent (SPGD) algorithm [9]. SPGD is a hill climbing-based algorithm which requires no phase knowledge, no reference waveform, and only a single detector; it thus greatly simplifies the overall architecture. During the beam steering cycle, commercial $LiNbO_3$ phase modulators are used to steer the beam by applying a time-varying phase profile across the elements. Due to the power scalability of the SCOWAs and the fast response time of the phase modulators, this system can be readily scaled to multi-watt class output and GHz steering speed.

Section 2 describes the methods used in this experiment for phase-locking, beam steering, and system characterization. Section 3 presents the results of SCOWA output power measurements, a near-ideal profile of a phase-synchronized beam to demonstrate the effectiveness of the phase-locking mechanism, and beam steering profiles at low (5 Hz) and high (40 MHz) steering speeds using different measurement methods.

2. Experimental setup

2.1. Schematic

Figure 1 is a schematic of the implemented master-oscillator-power-amplifier (MOPA) architecture. A 100 mW, fiber-coupled, isolated, narrow-linewidth (8 MHz at 1064 nm) seed (Photodigm DBR laser) is split and sent into 6 phase modulators used for beam steering. Outputs from the phase modulators are then amplified by a one-dimensional SCOWA array biased at 700 mA per element. The SCOWA array is a 7-element array with one defective interior element and can thus be considered a 6-element unequally-spaced array. In order to maintain proper polarization alignment, polarization-maintaining (PM) fibers were used throughout the

#167785 - $15.00 USD Received 1 May 2012; revised 8 Jun 2012; accepted 12 Jun 2012; published 16 Jul 2012

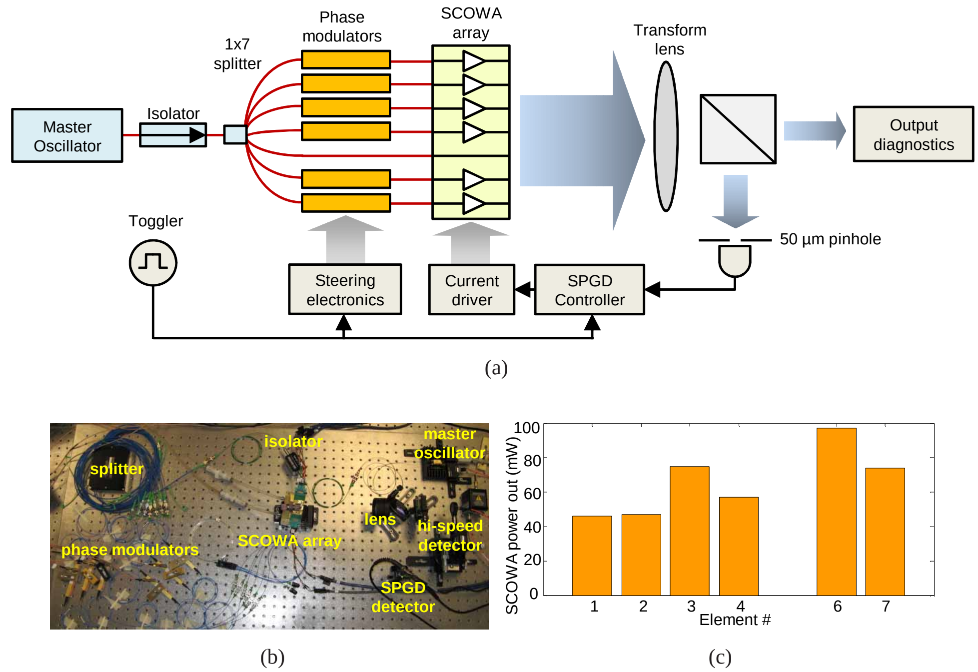

Fig. 1. (a) System schematic. (b) Photo of optical assembly. (c) Measured power emitted by SCOWA array.

system and were aligned to the SCOWA waveguides, which have gain only for TE modes polarized parallel to its quantum wells. The output facet of the SCOWA waveguides is angled to prevent back-reflection and potential parasitic lasing. The SCOWA array output is collimated by a transform lens positioned a focal length away. A pinhole samples the on-axis far-field intensity with a silicon photodetector (Thorlabs PDA100) and sends the electrical signal into the SPGD controller [10]. The SPGD controller dithers the phase of the elements at 1 kHz dither frequency to determine the appropriate phase correction needed to maximize on-axis intensity. The phase dithers are actuated by current modulation of the SCOWA elements. Figure 2(a) shows a trace of the on-axis intensity as SPGD is turned on. The zoomed-in plot shows a ∼30 ms convergence time, which is defined as the duration beyond the onset of SPGD for the on-axis intensity to converge to 90% of the maximum value. The SPGD algorithm was implemented in a software program on a personal computer operating a real-time Linux operating system. With a dither frequency of 1 kHz, the computer controls the 6 ILX Lightwave current drivers that power the SCOWA array. Table 1 lists the parameters of the experimental system.

2.2. *Toggling*

Due to the non-common opto-mechanical phase drifts caused by thermal and acoustic noise in the fibers, the length of time in which open loop steering can be performed is limited to ∼200 ms. Beyond this time, the phase drift causes the on-axis intensity to drop below 75% of the peak, as shown in Fig. 2(b). To re-lock the phases, the SPGD algorithm performs a maintenance cycle, during which steering is temporarily disabled. After the maintenance cycle, open loop steering is reinitiated. We refer to this operation as toggling between two different cycles: SPGD phase-lock cycle and open loop beam steering cycle. Figures 2(c) and 2(d) illustrate the toggling operation.

#167785 - $15.00 USD Received 1 May 2012; revised 8 Jun 2012; accepted 12 Jun 2012; published 16 Jul 2012

Table 1. Parameters for experimental system.

Parameter	Value
Array number	6 (7-element array with 1 dead element)
Emitter aperture	6 μm
Array pitch	250 μm
Fill factor	1/42
FWHM lobe width	565 μrad (0.0324°)
Steering range (limited by grating lobe spacing)	4.2 mrad (0.24°)

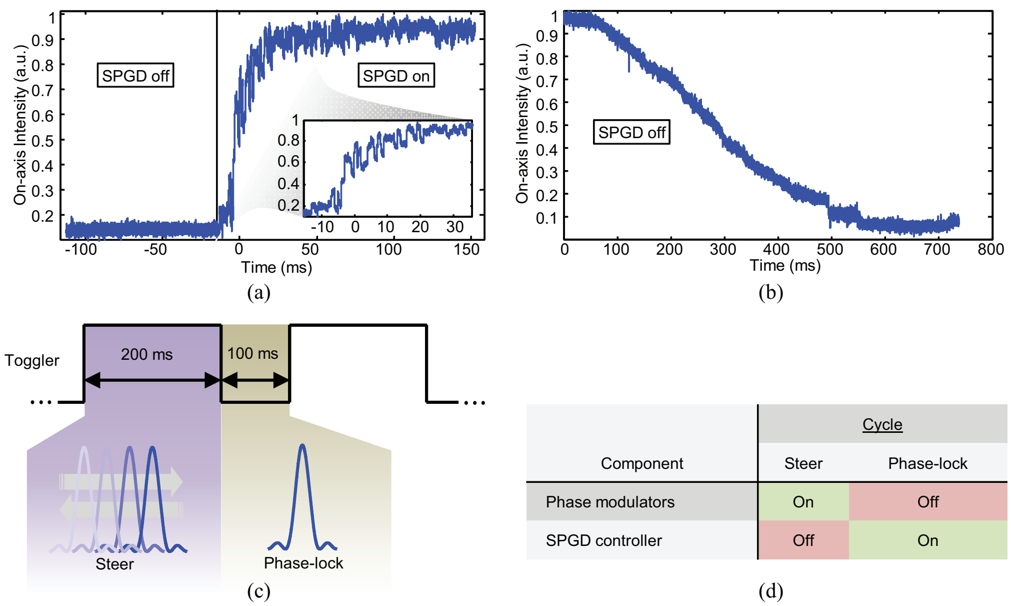

Component	Cycle: Steer	Cycle: Phase-lock
Phase modulators	On	Off
SPGD controller	Off	On

Fig. 2. (a) Phase-lock convergence trace. (b) Dephasing trace (SPGD is turned off at $t = 0$). (c) Illustration of toggling modality. (d) Table describing on-off operation of components during steer and phase-lock toggling cycles.

During the phase-lock cycle, the phase modulators used for steering are turned off so that they do not interfere with the active feedback. To reliably achieve phase synchronization, the duration of the phase-lock cycle must be no shorter than the convergence time of SPGD. Based on the typical convergence time of 30 ms, we have set the phase-lock cycle duration to 100 ms, several times higher than 30 ms to ensure convergence. During the steer cycle, the active feedback of the SPGD controller is disabled, the SCOWA bias currents are held at the last values of the phase-lock cycle, and the phase modulators are turned on to initiate steering. The toggling is controlled by a square-wave signal sent as a digital on-off gate to the SPGD controller and concurrently as an amplitude modulation signal to the phase modulator control port.

2.3. *Phase dithers for SPGD*

During the phase-lock cycle, each SCOWA element's phase delay is dithered by slightly adjusting its bias current. The current-to-phase relationship was interferometrically measured to be 2 mA per $\lambda/80$ change in phase delay. Changes to the SCOWA bias current alter the phase

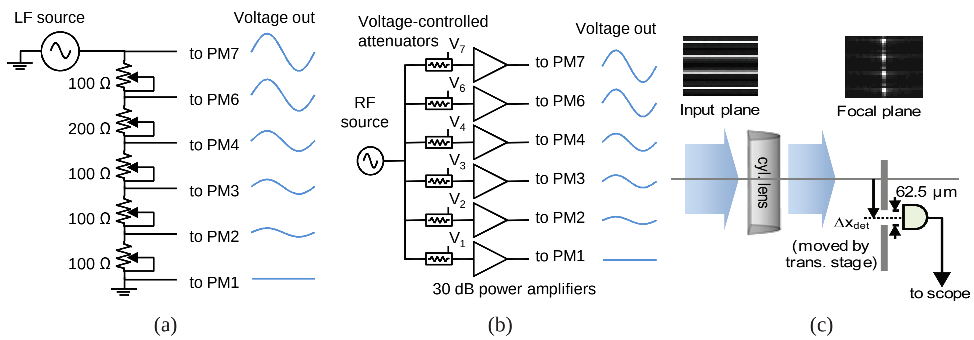

Fig. 3. (a) Electronics for driving the phase modulators (PM) for low frequency (LF) steering. (b) RF electronics for driving the phase modulators for RF steering. (c) Far-field diagnostics setup for RF steering.

by changing the refractive index via $\frac{dn}{dT}$. The small amplitude variation caused by adjusting the drive current has negligible effect on the beam combining efficiency [11].

2.4. *Phase modulators for steering*

During the steer cycle, each channel's phase delay is modulated by commercial $LiNbO_3$ phase modulators built by EO Space. These discrete, fiber-pigtailed devices measure $88.4 \times 8.9 \times 8.9$ mm^3 in size and the V_π's were measured to uniformly be 1.06 V. Because the devices were terminated by 50 Ω resistors, the P_π is 11.2 mW. To drive 6 phase modulators such that the beam steers sinusoidally over the steering range, the total power consumption to control the modulators is 190 mW. The devices have a modulation bandwidth of 10 GHz, allowing the scaling of the steering system to GHz operation.

2.5. *Steering electronics*

Beam steering is achieved by supplying a time-varying, spatially-linear voltage profile to the phase modulators. For low frequencies, a simple voltage divider suffices as shown in Fig. 3(a). However, in order to generate these voltages with fine amplitude control and phase uniformity at RF, custom drive electronics were designed and constructed as shown in Fig. 3(b). A 20 MHz RF source is split and sent through voltage-controlled variable attenuators, followed by 30 dB power amplifiers. The variable attenuators are tuned such that there is a spatially-linear voltage amplitude progression on the RF outputs. The output waveforms are then sent to drive the phase modulators.

2.6. *Diagnostics*

Beam steering is first demonstrated at low frequency (5 Hz) so that the beam profile could be captured by a 30 Hz, 10-bit CMOS camera (Coherent LaserCam). The camera is placed a focal length away from the transform lens and its integration time is adjusted with the peak pixel just under saturation to maximize dynamic range.

At RF steering frequencies, a different measurement method is required. Figure 3(c) shows the RF steering diagnostics setup. A fiber-coupled high-speed InGaAs detector (New Focus 1444) is used to measure the intensity as the beam transits across the aperture. The aperture is set by the 62.5 μm fiber tip. A cylindrical lens is used to compress the beam in the invariant vertical axis in order to increase the signal. In order to sample different portions of the steering range, the detector is moved horizontally by a translation stage.

3. Results

3.1. Power measurements

The aperture output power of each SCOWA element was measured by focusing into an optical power meter (OPHIR Vega). Figure 1(c) shows the output power of each element. Element 5 was non-emitting due to a fabrication defect. According to [11], the measured 30% power non-uniformity across the emitting elements causes only a 2.3% drop in the on-axis intensity compared to an array with uniform power; therefore, no attempt was made to correct for the power non-uniformity. The total output power from the SCOWA array was 396 mW. This power can be increased by increasing seed power or bias current. Finally, it is worth noting that there is no change in the power efficiency of the SCOWAs during steering operation because the output optical power is not affected by phase change.

3.2. Phase synchronized beam profile

The center portion of the phase synchronized far-field beam pattern was directly captured by camera, as shown in Fig. 4(a). The image shows vertical features due to the one-dimensionality of the array. The horizontal profile is plotted against the ideal phase synchronized pattern, which was numerically calculated by taking the Fourier transform of the aperture profile, assuming Gaussian profiles, equal phases, and non-uniform amplitudes given in Fig. 1(c). The agreement with theory indicates that the phase-locked loop achieves a high degree of phase synchronization. To quantify the phasing quality, the FWHM width broadening of the central lobe was measured. The width was measured to have increased by 5% from ideal, corresponding to a width of 565 μrad.

3.3. Low frequency steering

A linear voltage ramp was applied to the phase modulators over the 200 ms steer cycle and the 30 Hz camera collected time-resolved beam profiles over many cycles. The voltage amplitudes were adjusted using potentiometers such that the lobe travelled the entire steering range of 4.2 mrad. Figure 4(b) plots the beam profile for multiple values of the steer angle, $\Delta\phi$.

The beam profiles during low frequency steering in Fig. 4(b) show some degradation compared to the phase synchronized case in Fig. 4(a). The average measured pulse width increase was 7%, which corresponds to a width of 576 μrad. This additional phase degradation was caused primarily by potentiometer tuning errors in the voltage divider steering electronics.

3.4. High frequency steering

The beam steering at 40 MHz was characterized by placing a high-speed detector at different positions along the horizontal axis and sampling the intensity with respect to steer angle as the steer angle is modulated at RF. The voltage amplitudes were adjusted using voltage-controlled attenuators such that the lobe travelled the entire steering range. Figure 5(a) displays the steer angle modulated at 20 MHz with an peak-to-peak of 4.2 mrad, which is equal to the full steering range of the system. Figure 5(b) displays the detector measurements. As seen in the figure, the central lobe transits the detector at times when the steer angle is equal to the detector position, $\Delta\phi_{det}$. Based on these figures, the transit time across the detector is as short as 3 ns and it takes 25 ns to steer across the steering window, which corresponds to a 40 MHz steering speed. For clarity, the detector position has been displayed in the same angular units as the steer angle.

The phasing quality was again characterized by analyzing the pulse width increase. The average increase of 5% corresponds to a width of 565 μrad. These results indicate that, with

#167785 - $15.00 USD Received 1 May 2012; revised 8 Jun 2012; accepted 12 Jun 2012; published 16 Jul 2012

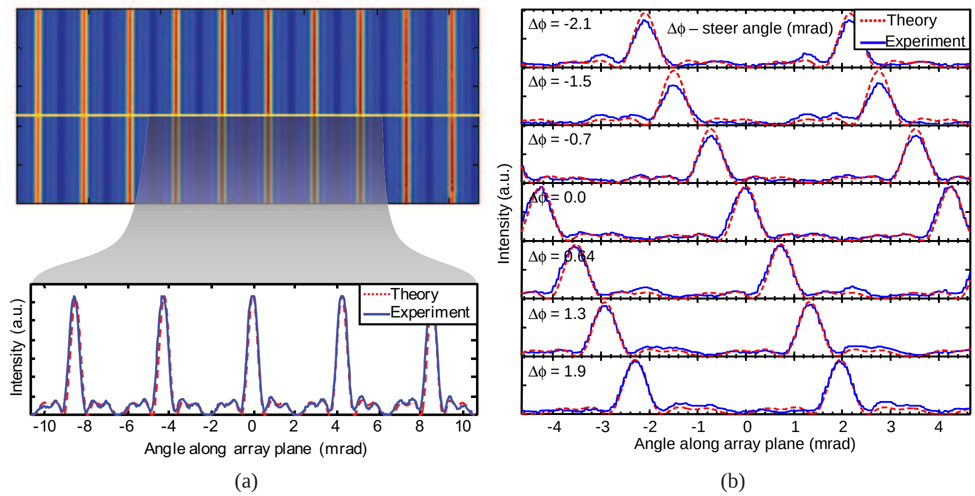

Fig. 4. Measured profiles of the central portion of the beam: (a) during phase synchronization and (b) during low frequency steering.

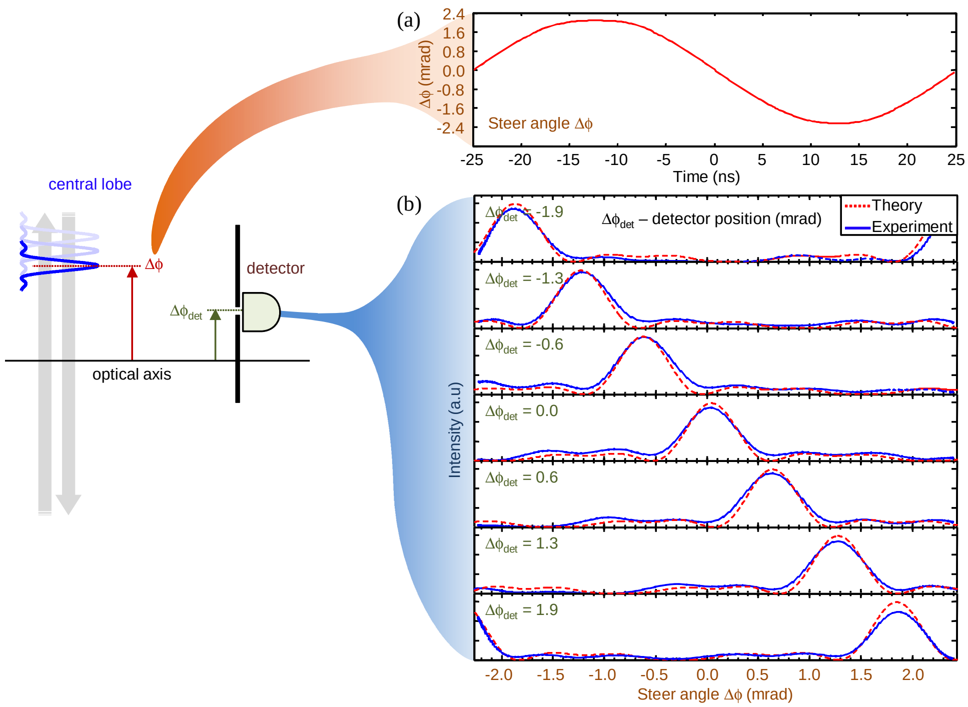

Fig. 5. High-speed detector measurements at RF steering. (a) The central lobe is deflected at 40 MHz steering speed by oscillating the steer angle, $\Delta\phi$. (b) These plots show the intensity on the detector versus steer angle as the central lobe transits through one steering period for different detector positions, $\Delta\phi_{det}$, along the steering direction.

#167785 - $15.00 USD Received 1 May 2012; revised 8 Jun 2012; accepted 12 Jun 2012; published 16 Jul 2012

the precise tuning capability of the voltage-controlled attenuators, minimal phase error was incurred from the steering mechanism.

4. Conclusion

This work reports fast steering speed from a 6-element optical phased array, with high power output, using coherent beam combining phase control techniques. Phase synchronization has been made possible through the SPGD phase-locking algorithm and the intrinsic stability of the SCOWAs; high speed beam steering has been made possible through custom-built RF electronics and fast $LiNbO_3$ phase modulators. Advantages to this design include fast steering speed, high power, and array scalability. Future work would include increasing the array fill factor by implementing a microlens array and scaling to more array elements. Anticipated results from this upgrade will include higher lobe intensity, narrower lobe width, and greater sidelobe suppression.

Acknowledgments

The authors acknowledge Richard Heinrichs for insightful comments, the DARPA MTO for the COCHISE program which made possible the SCOWA array development, Leo Missaggia for fabrication of the SCOWA array, Peter Foti for the construction of custom mechanical and electrical components, Kevin Creedon and Michael Taylor for fiber splicing work, and Andrew Benedick for useful discussions. This work was supported by the Assistant Secretary of Defense under the Air Force Contract FA8721-05-C-0002. Opinions, interpretations, conclusions, and recommendations are those of the authors, and are not necessarily endorsed by the United States Government.